

Original Research Article

Estimation of Regional Evapotranspiration based on Tri-Angle Method Using Thermal and VNIR Data.

Abstract

Evapotranspiration is a critical component in the hydrological cycle, water resources management and climate studies especially in arid and semi-Arid regions. Many remote sensing models proposed to estimate actual Evapotranspiration (ET_a), but it is more complicated and need to more surface and climate information. This paper aimed at producing a simplified, applicable and validated procedure for estimating spatial distributed daily actual evapotranspiration (ET_a) directly at regional scale to produce ET_a maps. Triangle method, which makes a parameterization of priestly-Taylor equation, was used to estimate ET_a at daily scale directly by using a simplified approach with realistic hypotheses. This study conducted in Egypt, Salhia, 6th of October Company as an arid region over the winter crops (wheat, potato and sugar beet) cultivated there using multi date Landsat images. The results were validated against ET_a values adjusted from crop evapotranspiration ET_c by using the Crop Water Stress Index (CWSI) approach. The results showed high accuracy and good agreement against assessment method. The correlation factor (R^2) values for wheat, potato and sugar beet were 0.88, 0.98 and 0.99 and Root Mean Square Error (RMSE) were 0.2, 0.26 and 0.37 respectively over the different dates of potato and sugar beet despite the late stage dates of wheat. In the 16th of April, there was a significant error as the RMSE were 0.8 and we explained the reasons of this error as it is a result of the sprinkler irrigation system effect on the mature wheat. This results show that the proposed procedure is accurate enough at least in most cases of our study for estimating the regional surface ET_a but it need to evaluate for wheat under other irrigation systems like surface or drip irrigation systems .

Keywords: Remote sensing, ET_a , Landsat, CWSI and Arid regions.

1. Introduction

Fresh water resources are becoming increasingly limited in many parts of the world, and decision makers are demanding new tools for monitoring water availability and rates of consumption (Martha, et al., 2012). The water shortage is the main constraint and a major limiting factor facing the implementation of the country's future economic development plans (Mohamed, et al. 2007). Global estimates of water consumption by sector indicate that irrigated agriculture is responsible for 85% of the water-use and that consumption in this sector will increase by 20% by 2025 (Droogers, et al. 2010). In general, Water availability is a major limitation for crop production and agriculture development specially, in arid and semi-arid regions. Egypt is under the water poverty line, as the per capita is less than 650 m³/year. In addition to water poverty, Egypt faces a great danger due to the millennium dam in Ethiopian, which will lead to water quota shortage from the Nile River. As the agriculture sector is the largest consumer of fresh water, so it will be the first and largest sector influenced by this shortage. Management water resources, developing irrigation systems, actual water requirements and its economic feasibility studies must be conduct in order to face this danger. A better understanding of the water balance

is essential for exploring water saving techniques. One of the most important concepts regarding water balance in arid and Semi-Arid areas is crop evapotranspiration (ET_c) which is a key factor for determining proper irrigation scheduling and for improving water use efficiency in irrigated agriculture (Er-Raki et al., 2007, Yang et al., 2011). Large volumes of water transfer from the soil and vegetation to atmosphere by evapotranspiration (ET). Accurate, spatially distributed information on water use, quantified at the scale of human influence, has been a long-standing critical need for a wide range of applications. Quantifying ET for irrigated crops in arid regions is vital to water resources management. The detailed ET maps enable managers to allocate available water precisely among agricultural, urban, and environmental uses. The actual rate of water use by vegetation can deviate significantly from potential ET rates due to impacts of drought, disease, insects, vegetation amount, phenology, soil texture, fertility and salinity (Anderson and Allen et al. 2012; Martha, et al., 2012). Different methods have been proposed for measuring ET on various spatial scales from individual plants to fields or landscape scales. However, conventional techniques provide essentially point measurements, which usually do not represent areal means because of the heterogeneity of land surfaces and the dynamic nature of heat transfer processes (Wang, et al. 2006; Wang & Dickinson, 2012). In recent years, as a result of the enormous developments in remote sensing technology, satellite data specifications, spatial, temporal and spectral resolution, are continuously improving. Many surface parameters, such as albedo, vegetation coverage, land surface temperature, and leaf area index, can be retrieved from visible, near-infrared, thermal infrared and other bands of satellite data. These data provide a basis for estimating ET from farmland and other regions and have attracted widespread attention for the use of remote sensing technologies to study regional ET (Li, X. et al., 2012). Over the last few decades, different physical and empirical remote sensing based models, which vary in complexity, accuracy, and needing for ancillary metrological data, have been proposed for estimating ET at different scales. In general, Accuracy in estimating ET basically depend on the accuracy of the input satellite data products, such as land surface temperature (LST), normalized difference vegetation index ($NDVI$), surface emissivity (ϵ_s) and surface albedo (α). However, the satellite derived variables are in turn and it depend on factors relating to residual atmospheric effects, spatial and temporal resolution, viewing angles, etc. Ancillary surface and atmospheric data like wind speed, aerodynamic resistance, and surface roughness, which cannot readily be measured through remote sensing techniques, usually required for these models. Therefore, it is still challenging to estimate and produce ET maps at regional and even global scale using satellite remote sensing without ground measurements or reanalyzed meteorological data. In order to overcome this problem, some attempts have been made to develop new parameterizations for ET estimation that depend entirely on remote sensing (Peng et al, 2013). One widely used approach among them is the LST - $NDVI$ triangle method, which was proposed by (Jiang and Islam 1999, 2001) and improved by (Jiang and Islam, 2003). Briefly, this method shows the relationship and the incident interaction between the soil, vegetation and weather conditions. The $NDVI$ values refer to the land cover type while, LST is a function in weather conditions and soil moisture content. This method is based on the P - T (Priestley-Taylor) equation (Priestley and Taylor, 1972), which can be considered as a simplified version of the more general Penman equation (Penman, 1948). The most sensitive point in this approach is the determination of the P - T parameter, which accounts for aerodynamic and canopy resistances and ranges from 0 at no ET to 1.26 at maximum ET . The P - T parameter is estimated from the triangular shape of the LST - $NDVI$ feature space, which is formed by the scatterplot of LST versus $NDVI$ over a wide range of soil moisture content and fractional vegetation cover. The

formalization of the triangular shape is caused primarily by different sensitivity of *LST* to soil moisture variations over bare soil and vegetated areas. There are several studies replaced the *NDVI* with other Vegetation Indices (*VI*) such as fractional vegetation cover (*Fr*) (Tang, et al. 2010; Liang, et al. 2011) or broadband surface albedo (Yang, et al. 2011). The advantages of *LST-VI* triangle method versus the other methods of surface energy balance for estimating *ET* are that:- 1) very high accuracy in *LST* retrieval and atmospheric correction are not indispensable, 2) needless to parameterize the complex aerodynamic resistance and uncertainty originated from replacement of aerodynamic temperature with *LST* is by passed, 3) it depends completely on remotely sensed *LST* and *VI*, 4) a direct calculation of evaporative fraction (*EF*), and 5) estimations of the Evaporative Fraction (*EF*) and the Net Radiation (*Rn*) are independent from each other. Therefore, the overall errors in *ET* can be traced back to *EF* and *Rn* separately. There are some other methods making the estimation of *EF* and *Rn* dependent on each other (Bastiaanssen, 2000; Norman et al. 1995), thus making it impossible to trace errors separately. Limitations of *LST-VI* triangle mainly lie in a bit subjective determination of both dry and wet edges and a large number of pixels required over a flat area with a wide range of soil moisture and fractional vegetation cover (Tang, R. et al. 2010). The triangle method has been applied successfully in certain applications for estimation of both *ET* (Gillies et al., 1997; Jiang and Islam, 2001; Nemani and Running, 1989; Price, 1990; Roerink et al., 2000; Rasmussen et al. 2014) and soil moisture (Carlson et al., 1995b; Sandholt et al., 2002). The main objective of this study is estimating daily *ET_a* directly with no need to estimate the net radiation (*Rn*) and evaporative fraction (*EF*) instantaneously by using a simplified approach during the winter agriculture season in the different growth stages of the crops cultivated in the study area.

2. Materials and Methods

2.1 Study area description

El-Salhia project is located at the eastern part from Nile Delta as shown in (Fig. 1). The whole area of the project is about 13,800 ha. Two irrigation systems are used in the project; the sprinkler irrigation center pivot and the drip irrigation. The project has about 100 center pivot irrigation units. Each pivot unit irrigates an area of about 63.6 ha. The common pivots length in the project is about 450 meter.

The climate in study area is a dry arid according to Köppen Climate Classification System, where precipitation is less than 50% of potential evapotranspiration. Annual average temperature is over 18°C. The average rainfall is approximately 20 (mm/year). The maximum values of rainfall are registered in January with average values of 6.9 (mm). The average maximum values of temperatures reach 34.6°C in June while January represents the coldest month 19.0 °C. The minimum temperatures range between 8.0 °C in January to 21.5 °C in August.

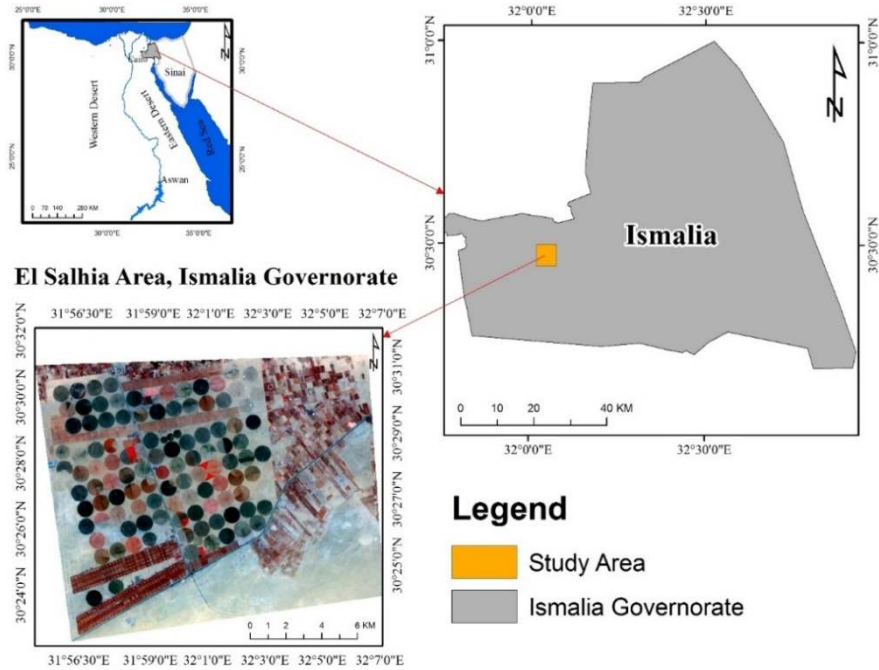


Figure (1) Location map of the study area.

2.2 Data availability

Satellite data: a combination of Landsat 7 and Landsat 8 (Path = 176 and Row = 39) were used to cover winter season crops. Table (1) illustrates the details of Landsat 7 and 8 satellite data.

Table (1) illustrates the Landsat 7 and 8 satellite data details.

No.	Date	Sensor type	Spatial resolution	Number of bands
1	17-12-2013	Landsat 7	30m×30m	8
2	02-01-2014	Landsat 7		8
3	11-02-2014	Landsat 8		11
4	15-03-2014	Landsat 8		11
5	31-03-2014	Landsat 8		11
6	16-04-2014	Landsat 8		11
7	02-05-2014	Landsat 8		11

Climatic metrological data: ground meteorological data namely air temperature, wind speed, dew point temperature and net radiation was used in order to calculate reference evapotranspiration (ET_o) during the days of the study.

2.3 ET_a estimation

The method applied here aimed to estimate daily ET_a directly by using the daily component of the energy balance equation eq.1;

$$R_n = G + H + \lambda E \quad (1)$$

Where; R_n is net radiation (Wm^{-2}), G is the soil heat flux (Wm^{-2}), H is the sensible heat flux (Wm^{-2}) and λE is the latent heat flux that is associated with the actual ET (Wm^{-2}). The energy balance can be rewritten to;

$$\lambda E = EF \cdot (Rn - G) \quad (2)$$

Where; EF is the dimensionless evaporative fraction and $(Rn - G)$ equals the net available energy for ET . G can often be ignored for time scales of 1 day or more, and thus λE is a function of Rn and EF only (Zwart et al. 2010). The EF is also defined as the ratio of actual ET to the available energy (dimensionless).

$$EF = \frac{\lambda E}{Rn - G} \quad (3)$$

The common formula which represents the Triangle method (Priestley and Taylor, 1972) was used in this study according to (Priestley-Taylor) equation;

$$\lambda E = \phi[(Rn - G) \frac{\Delta}{\Delta + \gamma}] \quad (4)$$

Where; ϕ is a $P-T$ parameter (PT), Δ is the slope of saturated vapor pressure at the air temperature (kPa/K) and γ is the psychrometric constant (kPa/K) and from eq. 2, 3 and 4, EF can be rewritten as;

$$EF = \frac{\lambda E}{Rn - G} = \phi \left(\frac{\Delta}{\Delta + \gamma} \right) \quad (5)$$

$LST-NDVI$ triangle method (Fig. 2) was applied. It is originated from the parameterization of (Jiang and Islam 1999), in a simplified $P-T$ formula (Priestley & Taylor, 1972). Regional ET_a and EF were estimated according to Eq. (4) which depends almost completely on remotely sensed data. The accurate interpreting of the scatter plot which resulted from remotely sensed LST and $NDVI$ under conditions of variance ranges of soil moisture availability and vegetation cover leads to accurate estimation of regional ET_a .

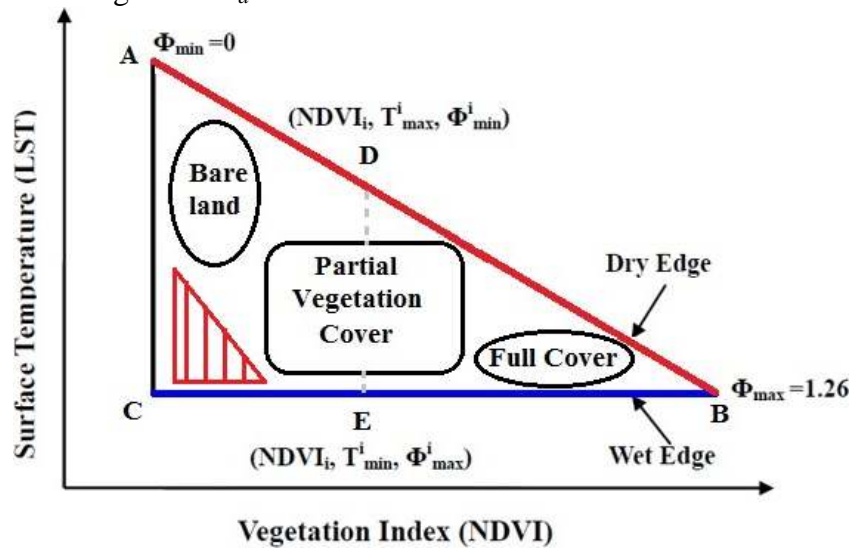


(Fig.2) Schematic diagram interpret the scatter plot of ($LST-NDVI$) triangular space to estimate evaporative fraction using wet and dry surfaces assumption and data distribution entire the triangle.

The dry edge is the oblique red solid line (AB) and the wet edge is the horizontal blue solid line (CB) represent the minimum ET and maximum ET , respectively. The two boundaries (dry and wet edges) of the $LST-NDVI$ feature space represent limiting conditions for the surface fluxes.

These edges respectively represent two limiting cases of soil moisture content and so evaporative fraction for each $NDVI$ value (i.e., the unavailability of soil moisture and stressed vegetation at the dry edge and non-stressed vegetation which evaporate potential ET at the wet edge). Specifically, EF at the wet edge is EF_{max} ($EF_{max}=1$) so, pixels at the wet edge are regarded to evaporate/transpire potentially while at the dry edge, EF varies from EF_{min} ($EF_{min}=0$) at the dry bare soil to EF_{max} ($EF_{max}=1$) at fully non stressed vegetation cover when availability of root zone soil water is good. At the dry edge, ET_a mainly comes from the transpiration of vegetation from the root zone water as the soil surface hasn't enough water to evaporate. The values of PT (ϕ) also ranges from ($\phi_{min} = 0$) at dry bare soil pixels to ($\phi_{max} = 1.26$) at non stressed with full vegetation cover pixels and the other ϕ values for each pixel are based on its soil water content and partial vegetation cover. In the absence of significant advection and convection, ϕ in eq. (4 and 5) can take a wider range of 0 (no ET) to $(\frac{\Delta+\gamma}{\Delta})$ (maximum ET).

Determination of dry and wet edges in the $LST-NDVI$ scatter is necessary, to estimate pixel by pixel ET and EF using Eqs. (4) and (5). In arid and semi-arid areas, it should be noted that, for given vegetation cover, spatial pixels with high surface temperature and low EF are detectable by satellite remote sensors. On the other hand, the saturated soil water which evaporates potentially pixels is rarely and hardly existed in these conditions (see red lined triangle inside fig.2).

Obtaining of the ϕ value for each pixel requires a three step linear interpolation scheme based on the $LST-NDVI$ triangle which used to allocate ϕ values inside the scatterplot (Fig. 2); (1) determines the dry and wet edges in the triangular space. The EF estimation accuracy depends basically on the accuracy of determining wet and dry edges; (2) minimum and maximum ϕ are respectively set to $\phi_{min} = 0$ for the driest bare soil pixel "with lowest $NDVI$ and highest LST " (point A) and $\phi_{max} = 1.26$ for the full vegetated pixel "with largest $NDVI$ and lowest LST " (point B). For each $NDVI_i$ value, there are max and min values of ϕ_i , $\phi_{i_{max}}$ located on the wet edge (point E) ($\phi_{i_{max}}$ is generally set to $\phi_{i_{max}} = \phi_{max} = 1.26$) and $\phi_{i_{min}}$ Located on the dry edge (point D). 3) Finally, ϕ_i entire each $NDVI$ value, is linearly interpolated between $\phi_{i_{min}}$ and $\phi_{i_{max}}$ through the similarity between the ABC and EBD triangles (Fig. 2). The following relation is taking out from the similarity;

$$\frac{AD}{AB} = \frac{ED}{AC}$$

Thus, by converting the symbols into real parameters, ϕ value for each pixel can be calculated using the given mathematical expression as follows;

$$\phi_i = [(\frac{T_{max}-T_i}{T_{max}-T_{min}})*(\phi_{max}-\phi_{min})] + \phi_{min} \quad (6)$$

Since the ϕ_{min} is equal to zero and ϕ_{max} is equal to 1.26, the eq.6 becomes as:

$$\phi_i = (\frac{T_{max}-T_i}{T_{max}-T_{min}})*1.26 \quad (7)$$

The above scheme accuracy depend on the accurate determination of the dry and wet edges, as the eq.7 depends on T_{max} which represents the high value on the dry edge and T_{min} which represents the wet edge as optimal conditions for ET . Also, intensive care during the pre-processing and extracting the LST from the remote sensing data must be taken into account.

(Fig.3) represents of the relation between *LST* and *NDVI* for sample of our data which illustrates the triangle shape and both of dry edge (oblique red line) and wet edge (horizontal blue line).

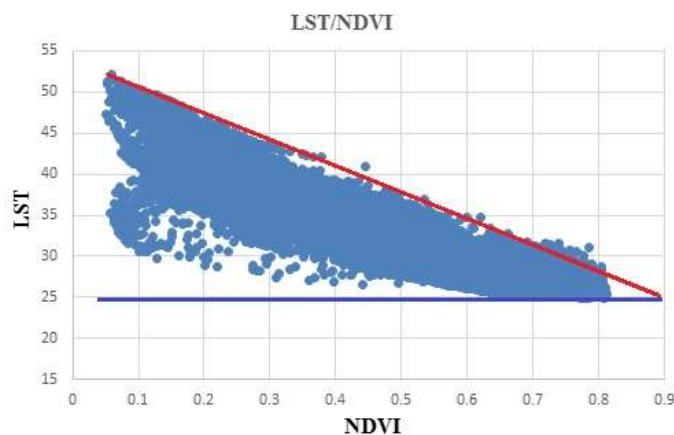


(Fig.3) Scatterplot which illustrates the triangle shape and both of dry edge (oblique red line) and wet edge (horizontal blue line).

(Bastiaanssen, 2000) and (Allen, 2001) used the (De Bruin, 1987) equation to calculate the daily (24 hours) R_n according to next formula;

$$R_{n24} = (1-\alpha)Rs_{\downarrow} - 110\tau_{sw24} \quad (8)$$

Where; R_{n24} is the daily net radiation (wm^{-2}), α is the surface albedo, Rs_{\downarrow} is the 24hour solar radiation (wm^{-2}) and τ_{sw24} is the atmospheric transmissivity.

The following assumption was used to estimate daily *ET* values in a direct way; the near noon instantaneous *EF*, which estimated by the triangle method was used as a representative value to the daily average *EF* value based on the observations of (Caparrini et al., 2004 and Crago, 1996) for both homogeneous and heterogeneous land surfaces *EF* remains fairly constant for daylight hours, particularly at about 10:00 and 16:00 O'clock and this assumption used by (Peng et al, 2013). During daytime, *EF* is mainly controlled and determined by land surface properties such as vegetation amount, soil moisture and surface resistance to heat and momentum transfer. Most of them are slowly varying parameters during daytime as compared to other fast changing variables (e.g., surface temperature and radiation), which have much stronger diurnal cycles due to radiation and atmospheric forcing (Jiang et al., 2009). On the other hand, analysis of our hourly climate data showed that the difference between meteorological parameters such as air temperatures and relative humidity at the satellite overpass time and the daily average of these parameters were not considerable. The highest relative error value of air temperature and relative humidity values during the overpass time value and the average daily value was not exceed 9.8% and 15% respectively over the seven used dates of data. Hence, we can regard the weather conditions during the satellite overpass time are representative of the whole day and *EF* too. In addition to, several studies have concluded that using local near noon *EF* instead of daily *EF* for daily *ET* estimation incurs very small error (Farah et al., 2004; Hall et al., 1992; Hoedjes et al., 2008; Jia et al., 2009).

$$ET_{daily} = (R_{n\ daily} - G_{daily}) * EF_{daily} \quad (9)$$

As the daily G ignored in this study, as it is usually assumed negligible over the diurnal cycle or day time scale (Sánchez et al., 2008; Jiang et al., 2009; Tang et al., 2011; Galleguillos et al., 2011). The above equation can be rewritten as;

$$ET_{\text{daily}} = (R_{\text{n daily}} * EF_{\text{daily}}). \quad (10)$$

2.4 Validation

Crop Evapotranspiration (ET_c) has been used to check the performance and the results of the proposed procedure by converting it from ET_c to actual ET_a using the crop water stress index ($CWSI$) extracted from satellite images. ET_c calculated by multiplying FAO table crop coefficient (K_c) and reference ET_o which calculated by using FAO-Penman-Monteith (FPM) equation. The $CWSI$ is based on observed canopy-air temperature differences and is an index for the water availability in the soil. When a crop with full cover has adequate water it will transpire at the potential rate for that crop. The actual evapotranspiration ET_a rate will fall below the potential rate when water becomes limiting (Jackson et al. 1981; Boegh et al. 2002; Boulet et al. 2007; Kustas et al. 2003a). The $CWSI$ ranges from 0 (no stress) to 1 (maximum stress) and has been defined as:

$$CWSI = 1 - (ET_a / ET_c) \quad (11)$$

The following expression used to calculate $CWSI$ as a function in difference in LST .

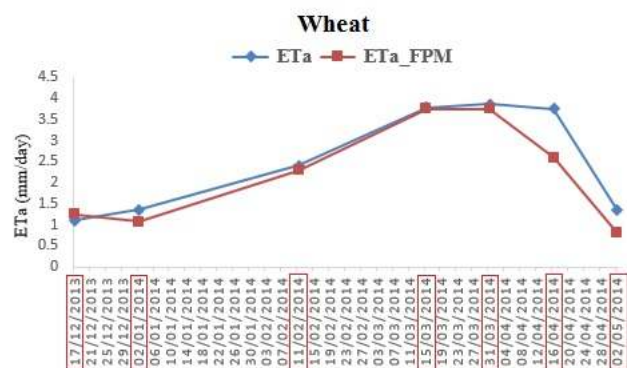
$$CWSI = \frac{(T_i - T_{min})}{(T_{max} - T_{min})} \quad (12)$$

Where; T_i is the LST of each pixel, T_{min} is the minimum LST , T_{max} is the maximum LST at the study area. This strategy was applied to verify the accuracy of the results of this approach on the wheat, potato and sugar beet crops during the different growth stages.

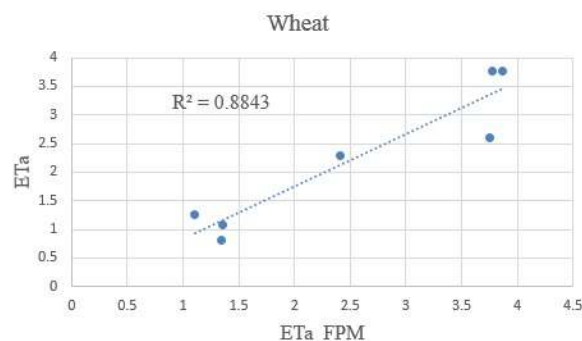
3. Results and Discussions

Daily ET_a was calculated by using eq.10, which consist of two main components EF and R_n . EF estimated by triangle method, which parameterize ($P-T$) parameter from the $LST/NDVI$ scatter plot. $P-T$ parameter (ϕ) is a down samples coefficient for both aerodynamic and surface resistance of evaporation and making the complicated sensible heat calculations are not needed the thing which make this procedure is more simple than others models. The $P-T$ parameter basically depends on and estimated by using LST in a form of rational equation which eliminates the error in LST calculation “if there is error”. There are other parameters in eq.5 which entered in calculation of EF such as Δ and γ which depend on air temperature. In this study, we used the air temperature which obtained from the metrological station in order to calculate the Δ and γ , but there are many studies aimed at correlate the LST and T_{air} in order to dispense of metrological information completely. The second component is the net radiation R_n , which estimated by using eq.8 at daily scale directly rather than instantaneous calculations. ET_a estimated by the proposed procedure validated against actual ET_a adjusted from ET_c by using the $CWSI$ which account for the soil moisture availability. Wheat, potato and sugar beet are three herbaceous crops which were used to test the validity of this procedure. The results showed high agreement and responsible results during different growth stages over these crops. The R^2 values of wheat, potato and sugar beet were 0.88, 0.98 and 0.99 respectively which mean that the proposed procedure had enough accuracy for wheat, potato and sugar beet at least in our case.

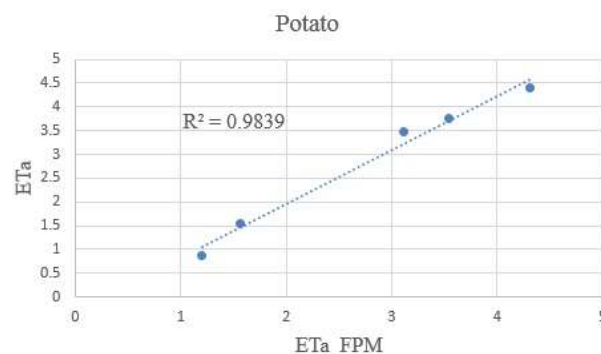
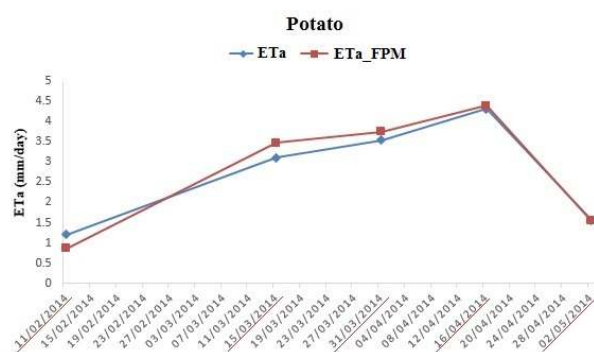
284



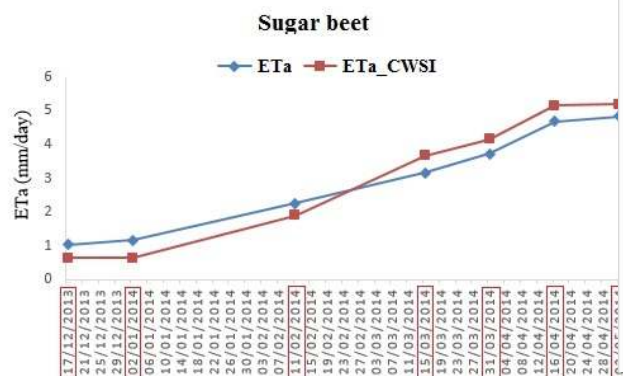
285



286



287



288

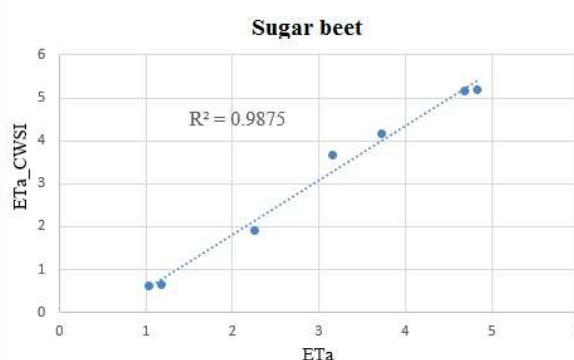
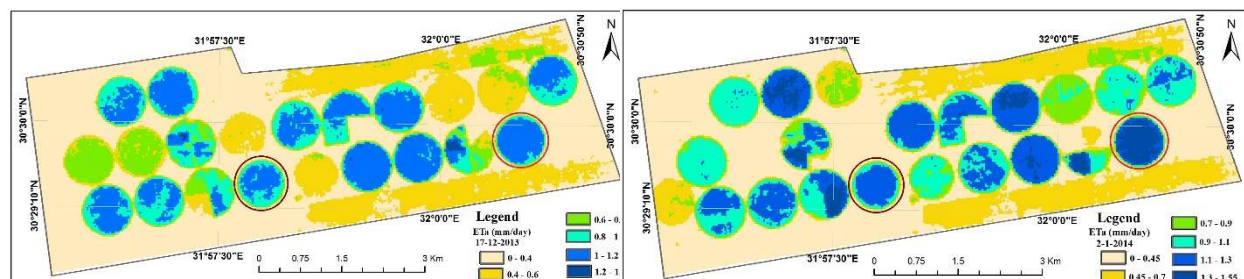


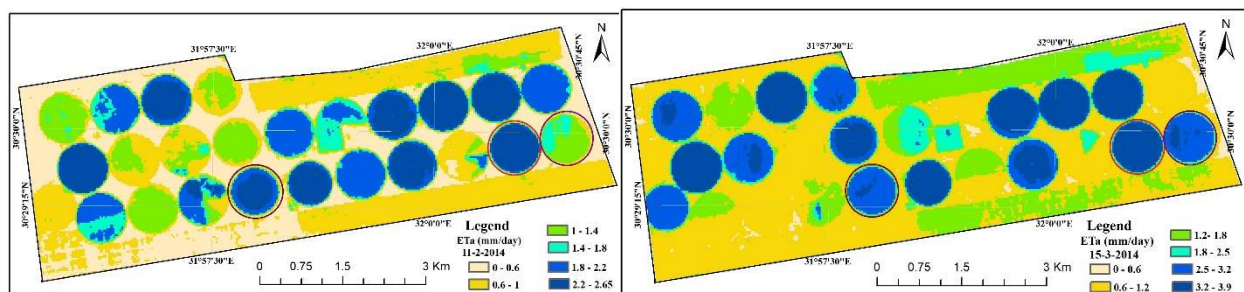
(Fig.4) shows matching and the correlation between the triangle method values and the validation method values for many crops which cultivated in the study area during different growth stages (highlighted dates on X axis are acquired satellite images dates).

Maps of daily *ETa* were created for all study area crops but for better view, we viewed a part which contains the studied center pivot units of the different crops in fig.5 and detailed *ETa* distribution for these crops (wheat, potato and sugar beet) at different crop stages in fig.6. The highlighted red, purple and brown circles represent wheat, potato and sugar beet respectively. In 17th of December the *ETa* values for wheat and sugar beet were 1.1 and 1 mm/day respectively and the validation values for these crops at the same date were 1.24 and 0.63 mm/day respectively. These values showed good agreement as the wheat and sugar beet where the RMSE

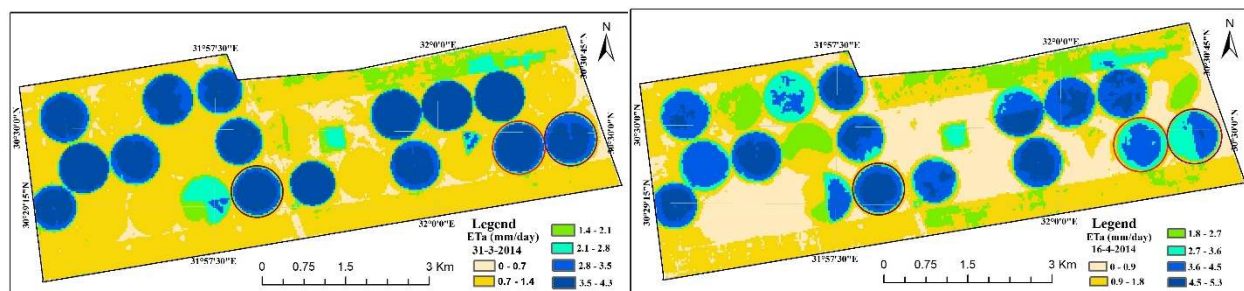
299 were 0.101 and 0.277 respectively. In 2nd of January, the *ETa* values for wheat and sugar beet
300 were 1.35 and 1.17 *mm/day* respectively and the validation values for these crops at the same
301 date were 1.07 and 0.65 *mm/day* respectively. These values showed good agreement as the wheat
302 and sugar beet where the RMSE were 0.201 and 0.37 respectively. In 11th of February, the *ETa*
303 values for wheat, potato and sugar beet were 2.41, 1.2 and 2.25 *mm/day* respectively and the
304 validation values for these crops at the same date were 2.29, 0.86 and 1.9 *mm/day* respectively.
305 These values showed good agreement as the wheat, potato and sugar beet where the RMSE were
306 0.079, 0.23 and 0.24 respectively. In 15th of March, the *ETa* values for wheat, potato and sugar
307 beet were 3.78, 3.1 and 3.16 *mm/day* respectively and the validation values for these crops were
308 3.76, 3.48 and 3.67 *mm/day* respectively. These values showed good agreement as the wheat,
309 potato and sugar beet where the RMSE were 0.013, 0.26 and 0.36 respectively. In 31th of March,
310 the *ETa* values for wheat, potato and sugar beet were 3.87, 3.54 and 3.72 *mm/day* respectively
311 and the validation values for these crops at the same date were 3.75, 3.75 and 4.16 *mm/day*
312 respectively. These values showed good agreement as the wheat, potato and sugar beet where the
313 RMSE were 0.079, 0.15 and 0.31 respectively. In 16th of April, the *ETa* values for wheat, potato
314 and sugar beet were 3.75, 4.3 and 4.66 *mm/day* respectively and the validation values for these
315 crops at the same date were 2.6, 4.4 and 5.14 *mm/day* respectively. These values showed good
316 agreement for potato and sugar beet where the RMSE were 0.06 and 0.32 respectively, but for
317 wheat there was significant error as the RMSE was 0.81. In 2nd of May, the *ETa* values for
318 wheat, potato and sugar beet were 1.3, 1.55 and 4.83 *mm/day* respectively and the validation
319 values for these crops at the same date were 0.8, 1.55 and 5.2 *mm/day* respectively. These values
320 showed good agreement as the wheat, potato and sugar beet where the RMSE were 0.38, 0.004
321 and 0.25 respectively. For crop wheat, there were no significant error at the initial development
322 and mid stages, but at the late stage a high significant error appeared as the RMSE were 0.81 in
323 16th of April and 0.38 in 2nd of May. We interpreted the significant error at the late stage to many
324 reason: 1) at the late stage wheat leaves, especially basal leaves, became almost dead which
325 mean that the cell structure is more weak and able to water absorption than healthy leaves
326 (development and mid stages). 2) sprinkler irrigation system increase the leaves water absorption
327 chance. 3) Continuation of the irrigation process to later stages every day or at least day after
328 day. The previous reasons made the LST and surface albedo (α) down normal, the thing which
329 raise the EF and Rn values respectively. Rising of EF and Rn values led to raising of estimated
330 *ETa* value. Absence of this significant error with potato and sugar beet “ever green until harvest
331 crops” support our interpretation. This mean that the proposed method need to test for wheat
332 under other irrigation systems like surface or drip irrigation.



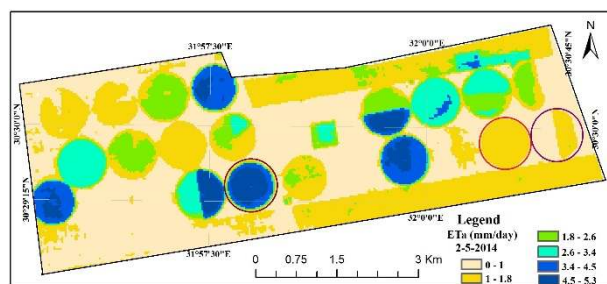
334



335



336



337

(Fig.5) distribution of daily ETa over different crops developing stages during the winter season



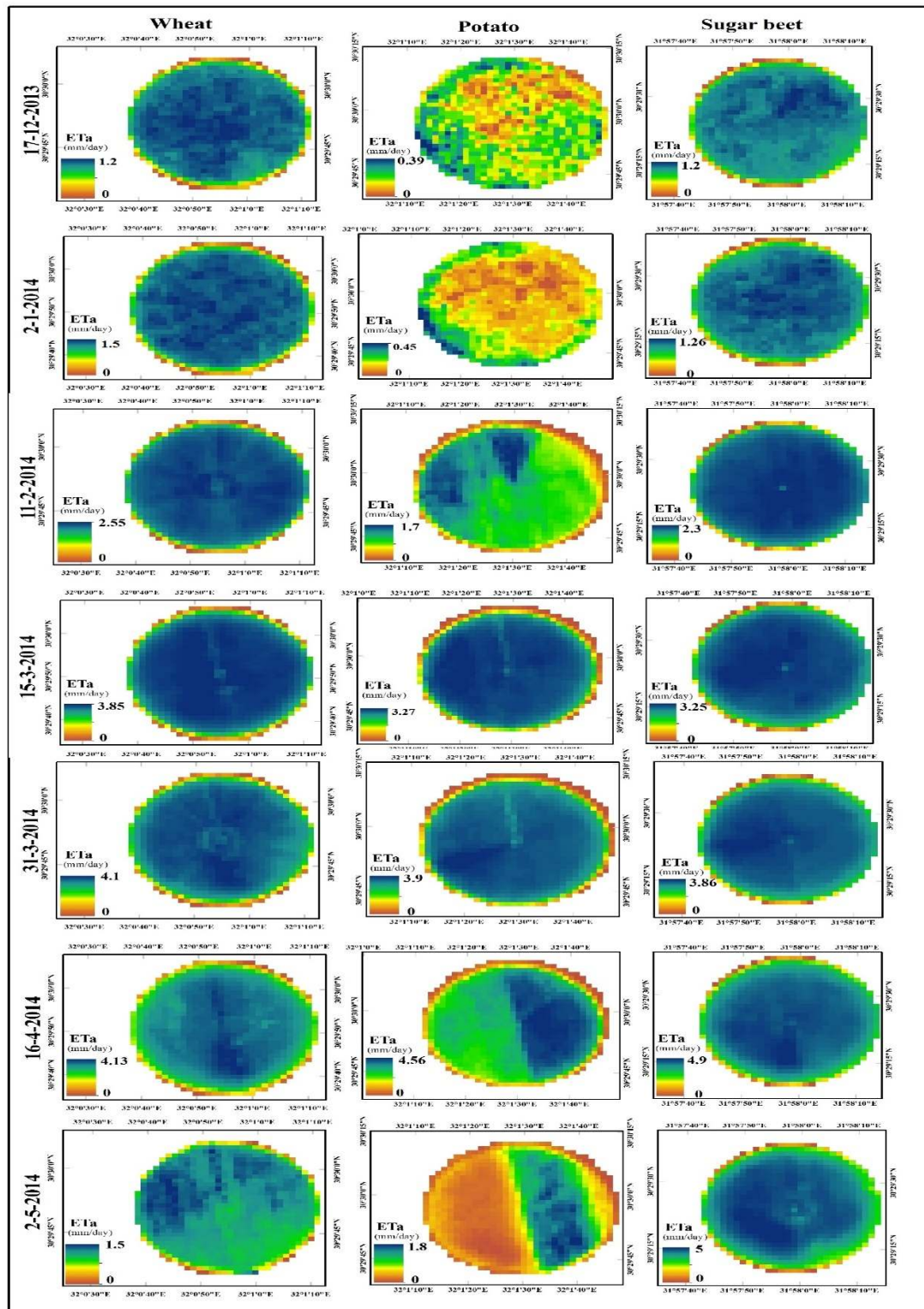


(Fig.6) ET_a distribution for wheat, potato and sugar beet crops which used for validation during different crop stages. (Note: on 17th of December, 2013 and 2nd of January, 2014, the potato Pivot was not cultivated)

342

343 4. Conclusion

344 Decision-makers and water resources managers are always need to regional information about
 345 *ET* to manage water resources distribution. Triangle remote sensing method was proposed by
 346 (Jiang and Islam 1999, 2001) and improved by (Jiang and Islam, 2003). This method is used for
 347 estimating spatial distributed regional *ET* and soil moisture content. Although, this method
 348 estimates instantaneous value of Evaporative Fraction (*EF*), it could be used to estimate daily
 349 *ET_a* directly; the near noon instantaneous *EF*, which estimated by the triangle method is used as
 350 a representative value to the daily average *EF* value which strengthened by the analysis of our
 351 climatic data. Actual *ET* at daily scale had been estimated directly for different dates during the
 352 winter season over different crops cultivated there. The assessment strategy conducted on three
 353 crops, wheat, potato and sugar beet through a comparison between *ET_a* estimated by the
 354 proposed procedure and *ET_a* adjusted from *ET_c* using the *CWSI* approach. *ET_c* calculated by
 355 using of *ET_o* from FAO Penman-Monteith (FPM) equation and FAO crop coefficient (*K_c*). The
 356 *ET_a* values of wheat varied from 1.1 mm/day at the development stage to 3.78 mm/day at the mid
 357 stage as the highest value, then 1.3 mm/day at the late stage. Potato graduated from 1.2 mm/day
 358 at the initial stage to 4.3 mm/day at the mid stage as the highest value, then 1.55 mm/day at the
 359 late stage. The last crop is sugar beet which graduated from 1 mm/day at the initial stage to 4.83
 360 mm/day at the mid stage. The maximum RMSE for the wheat (before the late season), potato and
 361 sugar beet is 0.20, 0.26 and 0.37 respectively over the different dates. At the late stage of wheat a
 362 high significant error appears due to the sprinkler irrigation system effect on the mature wheat.
 363 The results showed high agreement between the two methods values during the growing season
 364 of the three crops. The R^2 values were 0.88, 0.98 and 0.99 for wheat, potato and sugar beet
 365 respectively which mean that, this method is a responsible, realistic and acceptable for estimating
 366 daily *ET_a* at regional scale. We recommend that, the proposed method need to evaluate for wheat
 367 under other irrigation systems rather than sprinkler irrigation system.

368 5. Reference

- 369 Allen, R., G., Tasumi, M., Mores, A., Bastiaanssen, W.G.M., Kramber, W., J., Anderson, H., N.,
 370 (2001). [Evapotranspiration from landsat \(SEBAL\): Application in the U.S., proceedings of](#)
 371 [Annual Conference of the International Commission on Irrigation and Drainage, Seoul,](#)
 372 [Korea.](#)
- 373 Anderson, M. C., Allen, R.G., Morse, A., Kustas, W. P., (2012). [Use of Landsat thermal imagery](#)
 374 [in monitoring evapotranspiration and managing water resources. Remote Sensing of](#)
 375 [Environment 122: 50-65.](#)
- 376 Bastiaanssen, W.G.M., (2000). [SEBAL-based sensible and latent heat fluxes in the irrigated](#)
 377 [Gediz Basin, Turkey. J Hydrol \(Amst\) 229:87–100. doi:10.1016/S0022-1694\(99\)00202-4.](#)
- 378 Boegh, E., Soegaard, H., Thomsen, A., (2002). [Evaluating evapotranspiration rates and surface](#)
 379 [conditions using Landsat TM to estimate atmospheric resistance and surface resistance.](#)
 380 [Remote Sens Environ 79:329–343. doi:10.1016/S0034-4257\(01\)00283-8.](#)
- 381 Boulet, G., Chehbouni, A., Gentine, P., Duchemin, B., Ezzahar, J., Hadria, R., (2007).
 382 [Monitoring water stress using time series of observed to unstressed surface temperature](#)
 383 [difference. Agric For Meteorol 146\(3–4\):159–172.](#)

- Caparrini, F., Castelli, F., and Entekhabi, D., (2004). Estimation of Surface Turbulent Fluxes through Assimilation of Radiometric Surface Temperature Sequences, *J. Hydrometeorol.*, 5, 145–159.
- Carlson, T.N., Gillies, R.R., Schmugge, T.J., (1995b). An interpretation of methodologies for indirect measurement of soil water content. *Agric For Meteorol* 77:191–205.
- Crago, R. D., (1996). Conservation and variability of the evaporative fraction during the daytime, *J. Hydrol.*, 180, 173–194.
- De Bruin, H.A.R., (1987). From Penman to Makkink. In: Hooghart, J.C. (Ed.), *Proceedings and information: TNO Committee on Hydrological Research*, vol. 39. Gravenhage, The Netherlands, p. 5–31.
- Droogers, P., Immerzeel, W.W., Lorite, I.J., (2010). Estimating actual irrigation application by remotely sensed evapotranspiration observations. *Agricultural Water Management* 97:1351–1359.
- Er-Raki S., Chehbouni A., Guemouria N., Duchemin B., Ezzahar J., Hadria R., (2007). Combining FAO-56 model and ground-based remote sensing to estimate water consumptions of wheat crops in a semi-arid region. *agricultural water management* 87: 41–54.
- Galleguillos, M., Jacob, F., Prévot, L., French, A., and Lagacherie, P., (2011). Comparison of two temperature differencing methods to estimate daily evapotranspiration over a Mediterranean vineyard watershed from ASTER data, *Remote Sens. Environ.*, 115, 1326–1340.
- Gillies, R.T., Carlson, T.N., Cui, J., Kustas, W.P., Humes, K.S., (1997). A verification of the “triangle” method for obtaining surface soil water content and energy fluxes from remote measurements of the Normalized Difference Vegetation Index (NDVI) and surface radiant temperatures. *Int J Remote Sens* 18(15):3145–3166.
- Farah, H., Bastiaanssen, W., Feddes, R., (2004). Evaluation of the temporal variability of the evaporative fraction in a tropical watershed, *Int. J. Appl. Earth Obs. Geoinf.*, 5, 129–140.
- Hall, F. G., Huemmrich, K. F., Goetz, S. J., Sellers, P. J., Nickeson, J. E.,(1992). *Satellite Remote Sensing of Surface Energy Balance: Success, Failures, and Unresolved Issues in FIFE*, *J. Geophys. Res.*, 97, 19061–19089, doi:10.1029/92jd02189.
- Hoedjes, J., Chehbouni, A., Jacob, F., Ezzahar, J., Boulet, G., (2008). Deriving daily evapotranspiration from remotely sensed instantaneous evaporative fraction over olive orchard in semi-arid Morocco, *J. Hydrol.*, 354, 53–64,.
- Jackson, R.D., Idso, S.B., Reginato, R.J., Pinter, P.J., (1981). Canopy temperature as a crop water stress indicator. *Water Resour Res* 17:1133–1138.
- Jia, L., Xi, G., Liu, S., Huang, C., Yan, Y., and Liu, G., (2009). Regional estimation of daily to annual regional evapotranspiration with MODIS data in the Yellow River Delta wetland, *Hydrol. Earth Syst. Sci.*, 13, 1775–1787.
- Jiang, L., & Islam, S. (1999). A methodology for estimation of surface evapotranspiration over large areas using remote sensing observations. *Geophysical Research Letters*, 26, 2773–2776.
- Jiang, L., Islam, S., (2001). Estimation of surface evaporation map over southern Great Plains using remote sensing data. *Water Resour Res* 37:329–340.
- Jiang, L., & Islam, S. (2003). An intercomparison of regional latent heat flux estimation using remote sensing data. *International Journal of Remote Sensing*, 24, 2221–2236.

- Jiang L., Islam S., Guo W., Jutla A., Senarath s. , Ramsay H., Eltahir E., (2009). [A satellite-based daily actual evapotranspiration estimation algorithm over South Florida. Global and Planetary Change 67:62–77.](#)
- Kustas, W.P., French, A.N., Hatfield, J.L., Jackson, T.J., Moran, M.S., Rango, A., (2003a) [Remote sensing research in hydrometeorology. Photogramm Eng Remote Sensing 69\(6\):613–646.](#)
- Liang, S., Rui, S., Xiaowen, L., Huailiang, c., Xuefen, Z., (2011). [Estimating Evapotranspiration Using Improved Fractional Vegetation Cover and Land Surface Temperature Space. Journal of Resources and Ecology, 2\(3\): 225-231.](#)
- Li X., Lu L., Yang W., Cheng G., (2012). [Estimation of evapotranspiration in an arid region by remote sensing—A case study in the middle reaches of the Heihe River Basin. International Journal of Applied Earth Observation and Geoinformation, 17:85–93.](#)
- Martha, C. A., Richard, G. A., Anthony, M., William, P. K., (2012). [Use of Landsat thermal imagery in monitoring evapotranspiration and managing water resources. Remote Sensing of Environment , 122: 50–65.](#)
- Mohamed, N. A., Gamal, I. A., (2007). [Water Resources in Egypt:Future challeges and opportunities. International Water Resources Association Water International, Volume 32, Number 2, Pg. 205-218.](#)
- Nemani, R., Running, S.W., (1989). [Estimation of regional surface resistance to evapotranspiration from NDVI and thermal-IR AVHRR data. J Appl Meteorol 28:276–284.](#)
- Norman, J.M., Kustas, W.P., Humes, K.S., (1995). [A two-source approach for estimating soil and vegetation energy fluxes from observations of directional radiometric surface temperature. Agric For Meteorol 77:263–293.](#)
- Peng, J., Liu, Y., Zhao, X., Loew, A., (2013). [Estimation of evapotranspiration from MODIS TOA radiances in the Poyang Lake basin, China. Hydrol. Earth Syst. Sci., 17: 1431–1444.](#)
- Penman, H. L., (1948). [Natural evaporation from open water, bare soil and grass, P. Roy. Soc. London Ser. A, 193: 120–145.](#)
- Priestley, C. H. B., & Taylor, R. J. (1972). [On the assessment of surface heat flux and evaporation using large-scale parameters. Monthly weather review, 100:81–92.](#)
- Price, J. C. (1990). [Using spatial context in satellite data to infer regional scale evapotranspiration. IEEE Transactions on Geoscience and Remote Sensing, 28, 940–948.](#)
- Rasmussen, M. O., Sørensen, M. K., Wu, B., Yan, N., Qin, H., Sandholt, I., (2014). [Regional-scale estimation of evapotranspiration for the North ChinaPlain using MODIS data and the triangle-approach. International Journal of Applied Earth Observation and Geoinformation 31:143–153.](#)
- Roerink, G.J., Su, Z., Menenti, M., (2000). [S-SEBI: a simple remote sensing algorithm to estimate the surface energy balance. Phys Chem Earth, Part B Hydrol Oceans Atmos 25\(2\):147–157.](#)
- S´anchez, J. M., Scavone, G., Caselles, V., Valor, E., Copertino, V. A., and Telesca, V., (2007). [Monitoring daily evapotranspiration at a regional scale from Landsat-TM and ETM+ data: Application to the Basilicata region, J. Hydrol., 351, 58–70, doi:10.1016/j.jhydrol.2007.11.041, 2008.](#)
- Sandholt, I., Ramussen, K., Anderson, J., (2002). [A simple interpretation of surface temperature/vegetation index space for assessment of surface moisture status. Remote Sensing of Environment, 79, 213–224.](#)

- 475 Tang, R., Li, Z., Tang, B., (2010). An application of the Ts–VI triangle method with enhanced
476 edges determination for evapotranspiration estimation from MODIS data in arid and semi-
477 arid regions: Implementation and validation. Remote Sensing of Environment 114 : 540–
478 551.
- 479 Wang K., Li Z., Cribb M., (2006). Estimation of evaporative fraction from a combination of day
480 and night land surface temperatures and NDVI: A new method to determine the Priestley–
481 Taylor parameter. Remote Sensing of Environment 102: 293–305.
- 482 Wang, K.C., & Dickinson, R.E. (2012). A review of global terrestrial evapotranspiration:
483 Observation, modeling, climatology, and climatic variability. Reviews of Geophysics, 50,
484 RG2005, <http://dx.doi.org/10.1029/2011RG000373>.
- 485 Yang, J., Wang, Y., (2011). Estimating evapotranspiration fraction by modeling two-dimensional
486 space of NDVI/albedo and day–night land surface temperature difference: A comparative
487 Study. Advances in Water Resources 34 : 512–518.
- 488 Zwart, S., J., Bastiaanssen, W., G., M., Fraiture, C., Molden, D., G., (2010). WATPRO: A
489 remote sensing based model for mapping water productivity of wheat. Agricultural Water
490 Management 97: 1628–1636